Available online at www.sciencedirect.com
ScienceDirect
Physica A 387 (2008) 4417–4428
PHYSICA A
www.elsevier.com/locate/physa

Bursting synchronization in non-locally coupled maps

J.C.A. de Pontes[a], R.L. Viana[a,*], S.R. Lopes[a], C.A.S. Batista[b], A.M. Batista[b]

[a] *Departamento de Física, Universidade Federal do Paraná, 81531-990, Curitiba, Paraná, Brazil*
[b] *Departamento de Matemática e Estatística, Universidade Estadual de Ponta Grossa, 84032-900, Ponta Grossa, Paraná, Brazil*

Received 29 February 2008
Available online 8 March 2008

Abstract

Neuron activity presents two timescales, a fast one related to action-potential spiking, and a slow timescale in which bursting takes place. Bursting activity in neuron ensembles can be synchronized, meaning the adjustment of the bursting phases due to coupling. We investigated bursting synchronization in a non-locally coupled lattice using a two-dimensional map to describe neuron activity. The coupling involves all sites in a lattice, the corresponding strength decreasing with the lattice distance in a power-law fashion. We observed bursting synchronization for wide intervals of the coupling parameters. We also investigated the bursting synchronization of the ensemble with an external time-periodic signal applied to one or more selected neurons.

Keywords: Synchronization; Bursting neurons; Neural ensembles; Non-local coupling

1. Introduction

The brain consists of about a hundred specialized modules with different functions, each of them being a complex network itself. Each network unit, the neuron, receives excitatory inputs from a few thousands of other neurons [1]. An intensively studied model for artificial neural networks is the Hopfield model [2], in the form of a spin system, with a symmetric connectivity matrix describing synaptic activity and the state variable is discrete and binary, assuming only two possible states: active or idle [3]. However, there is no dynamical generation of information within a neuron in Hopfield-type models. This would be an interesting feature of artificial neural networks, since there is laboratory evidence that neuron dynamics can present periodic and chaotic behavior [4]. The use of continuous state variables in the network units is thus very appealing, provided there is some deterministic process governing its temporal evolution.

From a more fundamental point of view, such dynamical processes should be models with neurophysiological background, as the Hodgkin–Huxley [5], Fitzhugh–Nagumo [6] or Hindmarch–Rose differential equations [7]. However, since a large number of network units are necessary to perform numerical simulations, faster results can be achieved with discrete-time maps, regarded as caricatures of the essential dynamics expected to be obtained from

* Corresponding author.
E-mail address: viana@fisica.ufpr.br (R.L. Viana).

0378-4371/$ - see front matter © 2008 Elsevier B.V. All rights reserved.
doi:10.1016/j.physa.2008.03.002

more sophisticated models [8]. Coupled map lattices, for which the units are discrete-time maps with a continuous state variable, have been considered as candidates for artificial neural networks [9].

We are particularly interested in low-dimensional maps which can mimic the two distinct timescales present in neuronal activity (i.e., the evolution of the action potential) in cortical circuits: (i) a fast timescale characterized by repetitive spiking; and (ii) a slow timescale with bursting activity, where neuron activity alternates between a quiescent state and spiking trains [10]. A characteristic feature of cortical circuits is that they can produce common rhythmic bursting, while its individual neurons, when isolated, show irregular bursts [11]. Many mathematical models emulate this spiking–bursting behavior, ranging from differential equations [7] to discrete-time maps [12,13].

Effective neural network modeling demands consideration of coupling prescriptions which emulate desirable characteristics of neuron ensembles. While most theoretical works on coupled map lattices have been done on models with nearest-neighbor (local) interactions, the large connectivity of the biological neuronal networks calls for non-local couplings. The simplest model is a global coupling lattice, which considers the interaction of each site with the mean field of all the other sites, regardless of their position along the lattice.

However, these models cannot cope with the fractal dendritic branching characteristic of biological neural networks [14]. Such fractally coupled neuronal networks have been experimentally found in the visual cortex V1 of ferrets [15]. The fractally coupled lattice proposed by Raghavachari and Glazier in Ref. [16] assumes that the probability of existence of a connection between two neurons located at positions $\vec{r}_i$ and $\vec{r}_j$ is proportional to $|\vec{r}_i - \vec{r}_j|^{-\alpha}$, where α is an exponent characterizing the effective range of the interaction. The number of such connections within a D-dimensional sphere of radius r scales with $r^{D-\alpha}$, so the term fractal for this coupling scheme [17]. As α increases from zero to infinity the coupling scheme goes continuously from a global "mean-field" coupling to a nearest-neighbor coupling, respectively, the fractal coupling being the intermediate case.

The presence of synchronized rhythms has been experimentally observed in electroencephalograph recordings of electrical activity in the brain, in the form of an oscillatory behavior generated by the correlated discharge of populations of neurons across the cerebral cortex. The behavioral state alters the amplitudes and frequencies of these oscillations, such that high-frequency and low-amplitude rhythms tend to occur during arousal and attention; whereas low-frequency and high-amplitude activity occurs during slow-wave sleep [18].

Interacting bursting neurons can exhibit a form of synchronization whereby the units start bursting at approximately the same time [10]. The existence of a slow timescale in coupled bursting neurons enables us to define a phase and frequency (its time rate) for each of them, even when on the spiking timescale they behave asynchronously [19]. The adjustment of the bursting phases and frequencies of two or more neurons can be treated as an example of chaotic phase synchronization, which is the occurrence of a certain relation between phases of interacting systems, bursting neurons in our case, while the amplitudes (related to the spiking timescales) can remain chaotic and uncorrelated [20]. The transition to mutual chaotic phase synchronization in bursting neurons was shown to occur, if the coupling strength is large enough, for a global coupling [19] and a scale-free lattice where the neuron connectivity has a power-law probability distribution function [21].

Once a neuron ensemble exhibits bursting synchronization, it has been shown that it can also be synchronized with an external time-periodic harmonic signal. The latter is able to produce frequency locking such that the time rate of the bursting phases adjusts to the frequency of the external signal. This external bursting synchronization has been applied to a global mean-field lattice [19] and a scale-free network [21]. Another procedure of external control is the use of a delayed feedback signal [22].

In this paper we investigate bursting phase synchronization of neuron assemblies where each unit is characterized by a two-dimensional map which mimics the spiking–bursting activity. The coupling prescription is non-local, in the sense that the interaction between two neurons depends on the lattice distance as a power law. We studied the time evolution of the bursting phases and their time rates to characterize the transition to a phase synchronized state. Such a transition depends on the coupling parameters: the strength and effective range. Moreover, we analyze the synchronization of the neuron bursting evolution with an externally applied harmonic signal.

The remaining of this paper is organized as follows: in Section 2 we present the properties of the map describing neuron dynamics, as well as the definition of a phase for the bursting dynamics. Section 3 outlines the kind of coupling between neurons and some of its properties. Section 4 deals with the dependence of chaotic phase synchronization on the network properties using suitable numerical diagnostics. In Section 5 we consider the synchronization between the bursting phases of neurons and the driving phase provided by a time-periodic external signal. Our conclusions are left to the last section.

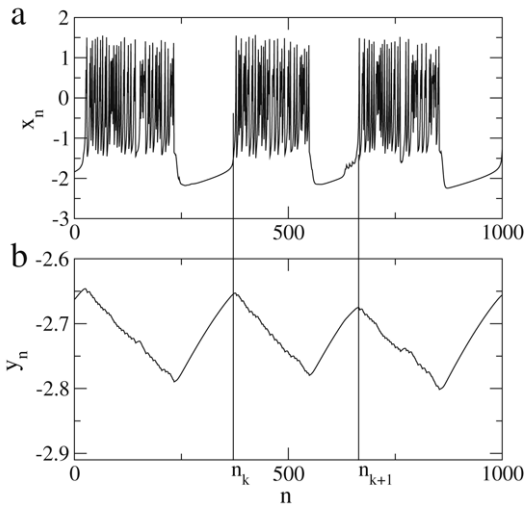

Fig. 1. Time evolution of the (a) fast and (b) slow variables in the Rulkov map (1)–(2) for $\theta = 4.1$, $\sigma = \beta = 0.001$.

2. Neuron dynamics and phase synchronization

We shall be concerned with neurons possessing two timescales, for there is a slow bursting modulating the fast action-potential spiking [23]. Such bursting neurons call for mathematical models consisting of three or more ordinary differential equations, like the Hindmarch–Rose equations [7] or discrete-time processes with at least two dimensions, like the map proposed by Rulkov [13]

$$x_{n+1} = \frac{\theta}{1 + x_n^2} + y_n, \tag{1}$$

$$y_{n+1} = y_n - \sigma x_n - \beta, \tag{2}$$

where x_n is the fast and y_n is the slow dynamical variable. The fast variable has a dynamical behavior emulating the spiking–bursting activity of a neuron, depending on the parameter θ, whereas the y-variable undergoes a slow evolution because of the small values taken on by the parameters σ and β, which model the action of an external dc bias current and synaptic inputs on a given isolated neuron [24].

We choose the parameter θ so as to yield chaotic behavior for the characteristic spiking of the fast variable x_n (Fig. 1(a)). The bursting timescale, on the other hand, comes about from the influence of the slow variable y_n. This can be understood by using a simple argument: since y_n represents a small input on the fast variable dynamics its effect can be approximated by a constant value γ. The resulting one-dimensional map, $x_{n+1} = [\theta/(1 + x_n^2)] + \gamma$, can have either one, two, or three fixed points $x^*_{1,2,3}$, depending on the value of the input γ. As the latter approaches a critical value γ_{SN} the fixed points $x^*_{1,2}$ (one stable and another unstable) undergo a saddle-node bifurcation, such that, for $\gamma \gtrsim \gamma_{SN}$, however, the fixed points $x^*_{1,2}$ disappear [13].

For values of $\gamma > \gamma_{CR}$ there is also a chaotic attractor that, provided $\gamma_{CR} < \gamma < \gamma_{SN}$, coexists with the stable fixed point attractor. Actually, at $\gamma = \gamma_{CR}$ the chaotic attractor collides with the unstable fixed point x^*_1 and is destroyed through a boundary crisis. The bursting regime comes from a hysteresis between the stable fixed point (quiescent evolution) and the chaotic oscillations (fast sequence of spikes) [8].

We consider a given burst to begin when the slow variable y_n, which presents nearly regular saw-teeth oscillations, has a local maximum, in well-defined instants of time we call n_k (Fig. 1(b)). The duration of the chaotic burst, $n_{k+1} - n_k$, depends on the variable x_n and fluctuates in an irregular fashion as long as x_n undergoes chaotic evolution. We can define a phase describing the time evolution within each burst, varying from 0 to 2π as n evolves from n_k to n_{k+1}:

$$\varphi_n = 2\pi k + 2\pi \frac{n - n_k}{n_{k+1} - n_k}, \tag{3}$$

where k is an integer. Since $n_{k+1} - n_k$ is different for each burst, it follows that the bursting phase rate also varies with time, such that we must look at the bursting frequency defined by

$$\Omega = \lim_{n\to\infty} \frac{\varphi_n - \varphi_0}{n}. \tag{4}$$

3. Non-locally coupled neuron ensembles

When the Euclidean distance between neurons does not play a significant role, the corresponding networks may be treated from a graph-theoretical point of view [25]. However, once we regard those neurons as embedded in a three-dimensional lattice (the brain, where they are connected by axons and dendrites), it is convenient to use a lattice embedded in an Euclidean space [26]. Considering an assembly of N neurons, each of them being described by the map (1)–(2), we reduce the neural network to a coupled map lattice, a procedure that has been used for a long time in theoretical and computational studies of neural activity [9]. One of the benefits of using this procedure is the need of less computer time in comparison with lattices of differential equations, what is particularly important if the number of neurons N is large.

Moreover, the investigation of non-local couplings is so difficult in lattices of high dimension that we consider simplified models consisting of one-dimensional chains. In a one-dimensional lattice let $(x_n^{(i)}, y_n^{(i)})$ represent the fast and slow variables for the neuron i ($i = 1, 2, \ldots, N$) at time n, such that the general form of the coupled map lattice is

$$x_{n+1}^{(i)} = \frac{\theta^{(i)}}{1 + \left(x_n^{(i)}\right)^2} + y_n^{(i)} + \mathcal{C}_n^{(i)}(x_n^{(j)}), \quad (j \neq i) \tag{5}$$

$$y_{n+1}^{(i)} = y_n^{(i)} - \sigma x_n^{(i)} - \beta. \tag{6}$$

In neuron ensembles some diversity in the biophysical parameters describing each unit is always expected. Hence we consider the parameter θ to be different for each site and taking on values in the interval $[4.1, 4.4]$, which produces chaotic behavior in the fast (spiking) timescale. The parameters σ and β, on the other hand, as describing the slow (bursting) timescale, are to take on small values only, and this value is the same for all neurons.

The coupling between neurons is performed only on the fast timescale by means of the term $\mathcal{C}^{(i)}$, the form of which depends on the network topology chosen to describe the neural network. When the degree of connectivity, i.e. the average number of connections per neuron, is large enough it has been usually chosen a global type of coupling

$$\mathcal{C}_n^{(i)}(x_n^{(j)}) = \frac{\epsilon}{N} \sum_{j=1}^{N} x_n^{(j)}, \tag{7}$$

where each neuron is coupled to the "mean field" generated by the entire lattice with strength $\epsilon > 0$. This form of coupling has been extensively used in studies of synchronization of bursting neurons [13,19]. However, since such a description does not take into account the dependence of the coupling on the distance between neurons, and the connectivity is the same for all neurons, the global coupling can only be considered as a simplified model.

In the power-law coupling it is possible to include the interactions among non-nearest neighbors in such a way that the coupling strength decreases as a power law with the lattice distance [27]

$$\mathcal{C}_n^{(i)}(x_n^{(j)}) = \frac{\epsilon}{\eta(\alpha)} \sum_{j=1, j\neq i}^{N'} \frac{1}{j^\alpha} \left[x_n^{(i+j)} + x_n^{(i-j)}\right], \tag{8}$$

where $\alpha > 0$ is a range parameter and

$$\eta(\alpha) = 2\sum_{j=1}^{N'} \frac{1}{j^\alpha}, \tag{9}$$

is a normalization factor, with $N' = (N-1)/2$ for N odd.

The coupling term in Eq. (8) is a weighted average of discretized second spatial derivatives, the normalization factor being the sum of the corresponding weights. If $\alpha \to \infty$, only those terms with $j = 1$ will contribute to the summations present in the coupling term, which results in $\eta \to 2$, or a Laplacian coupling, where a given site interacts only with its nearest neighbors. The latter coupling, however, is not suitable for describing neuronal networks. For $\alpha = 0$, on the other hand, we recover the mean-field coupling (7), such that we pass continuously from a local to a global coupling by varying the range parameter α. For intermediate values of α we have the same range dependence as in the model proposed by Raghavachari and Glazier to simulate a fractal (dendritic) coupling, in which the connections are randomly chosen according to a probability distribution which takes into account the distance between sites as a power law [16]. In our model the connections are strictly regular but follow the same dependence on the lattice distance.

4. Phase synchronization of bursting neurons

In order for the coupled map lattice (5)–(6) to exhibit a completely synchronized state, $x_n^{(1)} = x_n^{(2)} = \cdots = x_n^{(N)}$, $y_n^{(1)} = y_n^{(2)} = \cdots = y_n^{(N)}$, it would be necessary that the latter be a possible solution of Eqs. (5)–(6), stable under infinitesimal perturbations along directions transversal to this state. However, since the θ-parameter of each neuron is randomly sparkled inside a given interval, such a completely synchronized state is not possible.

This does not mean, however, that the system cannot present coherent behavior, since their bursting phases can synchronize through the interaction provided by the coupling architecture. If we had just two coupled neurons, chaotic phase synchronization imply simply that their phases be approximately equal, up to a given tolerance: $|\varphi_n^{(1)} - \varphi_n^{(2)}| < C \ll 1$. In the case of a large number N of systems, however, other diagnostics of phase synchronization need to be used. One such indicator is the mean field of the lattice,

$$M_n = \frac{1}{N}\sum_{j=1}^{N} x_n^{(j)}. \tag{10}$$

If the neurons are weakly coupled, they burst at different times in a non-coherent fashion, and the mean field fluctuates irregularly with small amplitudes. Contrarily, if the neurons burst synchronously (i.e. they start bursting at approximately the same times) a nonzero mean field is formed and M_n presents regular oscillations of comparatively large amplitude. Only the slow timescale dynamics becomes coherent as the neurons burst synchronously, and the fast timescale spiking remains incoherent and do not contribute to the mean-field dynamics, which is kept close to a periodic regime [19].

When the neurons are coupled in a global fashion (small α) and the coupling strength ϵ is large enough the mean field exhibits large-amplitude oscillations (Fig. 2(a)) since the neurons are bursting at approximately the same times, in spite of their spiking evolution being poorly or not correlated at all. This is best shown by Fig. 2(d) and (g) where we compare the time evolution of the fast variable for two different neurons (i.e., with different values of θ) belonging to the lattice, whose bursting times are nearly equal, which corresponds to a coherent output for the entire network.

By way of contrast, let us consider an assembly of neurons coupled in a local fashion (large α, where only the nearest neighbors contribute appreciably to the coupling). The corresponding mean field has small-amplitude noisy fluctuations (Fig. 2(c)) indicating that the neurons are not bursting in phase, as can also be seen by comparing the uncorrelated bursting activity of two selected neurons (Fig. 2(f) and (i)). That these two situations are limiting cases can be appreciated by looking at the mean-field evolution for an intermediate α-value (Fig. 2(b)), where the neurons burst at different, albeit near time instants (Fig. 2(e) and (h)).

Another aspect of the coherent behavior observed in this system is the synchronization of the neuron bursting frequencies (given by Eq. (4)), which is a direct consequence of their phase synchronization. When the neurons are uncoupled their unperturbed frequencies $\Omega_0^{(i)}$, being dependent on the fluctuating parameter θ, are likewise subjected to random fluctuations. One of the observed effects of coupling is the formation of synchronization plateaus with a constant value of the frequencies $\Omega^{(i)}$ for many sites characterized by different values of $\Omega_0^{(i)}$, though not necessarily correspondent to neighbor sites in the lattice. This behavior is illustrated in Fig. 3, where we plotted the frequencies $\Omega^{(i)}$ *versus* their zero-coupling counterparts $\Omega_0^{(i)}$ which, for the parameter values we adopted, take on values within the interval [0.0175, 0.0330].

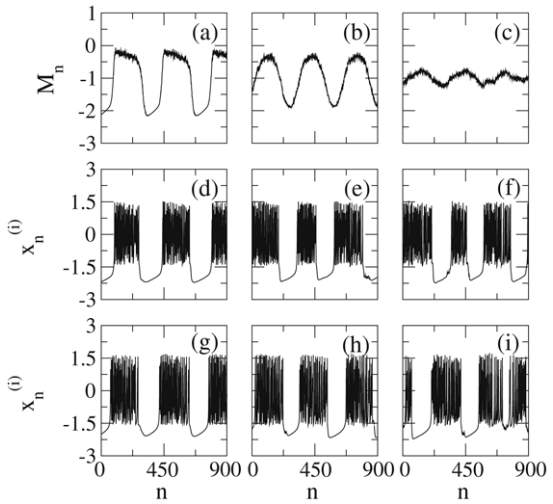

Fig. 2. Time evolution of the mean field for a non-locally coupled lattice of $N = 51$ Rulkov neurons with $\epsilon = 0.07$ and (a) $\alpha = 0.5$; (b) $\alpha = 2.0$, and (c) $\alpha = 4.0$. Time evolution of the fast variable of a coupled neuron for which $\theta^{(i)} = 4.2$ and (d) $\alpha = 0.5$; (e) $\alpha = 2.0$; and (f) $\alpha = 4.0$. (g), (h) and (i) stand for the coupled neuron for which $\theta^{(i)} = 4.4$ and the values of α are the same as in (d)–(f).

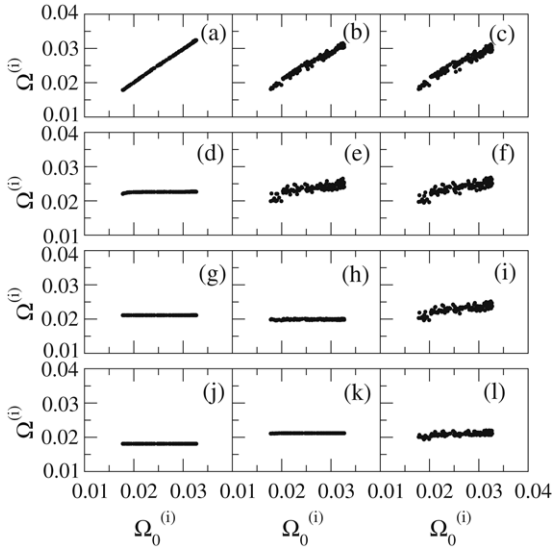

Fig. 3. Bursting frequency for the power-law coupled lattice with $N = 51$ and *versus* the zero-coupling frequencies for the following values of the coupling parameters (α, ϵ): (a) (0.5, 0.015); (b) (2.0, 0.015); (c) (4.0, 0.015); (d) (0.5, 0.035); (e) (2.0, 0.035); (f) (4.0, 0.035); (g) (0.5, 0.045); (h) (2.0, 0.045); (i) (4.0, 0.045); (j) (0.5, 0.07); (k) (2.0, 0.07); (l) (4.0, 0.07).

When the coupling strength is low enough there is no synchronization of bursting and the frequencies are distributed so as to have a linear trend $\Omega^{(i)} \approx \Omega_0^{(i)}$ (Fig. 3(a)). Keeping the α parameter fixed at 0.5 and increasing the coupling strength indeed leads to phase and frequency synchronization of bursts, the frequencies having been locked at values around 0.02, the actual value decreasing slightly with the coupling strength used (Fig. 3(d), (g), and (j)). This evolution is qualitatively the same for higher α, but frequency synchronization occurs earlier than in the previous case (Fig. 3(b), (e), and (h)). Moreover, the common frequency achieved for strong coupling reaches a higher value (just above 0.02) than it does for lower coupling (Fig. 3(k)). For even higher values of α, meaning local or nearest-neighbor coupling, it is clear that frequency synchronization does not occur (Fig. 3(c), (f), (i)), unless a very strong coupling is used and, even so, frequency locking occurs with some dispersion coming from the imperfect character of the phase synchronization (Fig. 3(l)).

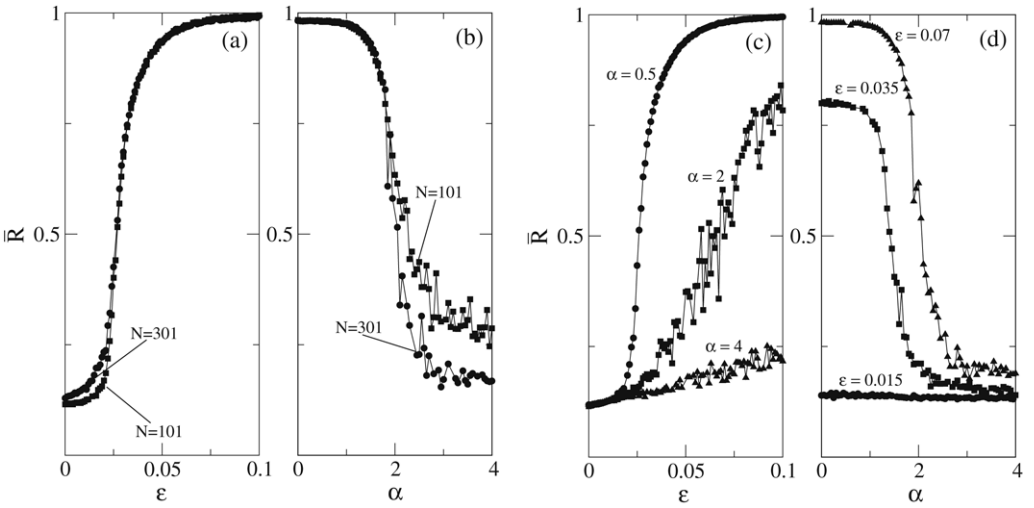

Fig. 4. Time-averaged order parameter for different values of N and as a function of (a) the coupling strength ε, with $\alpha = 0.5$; (b) the range parameter α, for $\epsilon = 0.07$. (c) The same as (a), but for $N = 231$ and three different values of α. (d) The same as (b), but for $N = 231$ and three different values of ϵ.

A more precise diagnostic of chaotic phase synchronization, though, is the complex phase order parameter defined by [28]

$$z_n = R_n \exp(\mathrm{i}\,\Phi_n) \equiv \frac{1}{N}\sum_{j=1}^{N} \exp(\mathrm{i}\varphi_n^{(j)}), \tag{11}$$

where R_n and Φ_n are the amplitude and angle, respectively, of a centroid phase vector for a one-dimensional lattice with periodic boundary conditions. If the bursting phases $\varphi_n^{(j)}$ are spatially uncorrelated their contribution to the result of the summation in Eq. (11) is typically small. On the other hand, in a completely phase synchronized state the order parameter magnitude asymptotes the unity, indicating a coherent superposition of the phase vectors for all sites with the same amplitudes R_n at each time.

This behavior is illustrated by Fig. 4(a), for fixed α and varying ϵ, where we plotted the time-averaged order parameter magnitude $\bar{R} = \lim_{T\to\infty} \frac{1}{T}\sum_{n=m}^{T} R_n$, the first $n = m - 1$ transient times having been discarded, and two different lattice sizes are considered. As expected, for uncoupled maps ($\epsilon = 0$) the order parameter takes on a small value (less than 0.2) due to poor coherence between bursting phases which actually decreases as the lattice gets larger. The order parameter increases rapidly with the coupling strength, approaching unity when ϵ is large enough, which indicates phase synchronization of the lattice, a feature already exhibited by the mean field (Fig. 2) and the bursting frequencies (Fig. 3). Assuming that for $N \to \infty$ the order parameter tends to zero for uncorrelated bursting, we can extrapolate the trends observed in Fig. 4(a) and locate a critical coupling strength $\epsilon_c \approx 0.024$, above which the lattice starts to synchronize, in the same fashion as a second-order phase transition of the type observed in the Kuramoto model (or globally coupled oscillators) [28]. However, this transition does not occur for any value of α, as exemplified by Fig. 4(c), where it fails to show up for higher α.

A similar situation can be described when the coupling strength ϵ is kept at a fixed value and range parameter α is varied (Fig. 4(b)). Globally coupled neurons are more likely to synchronize their bursting phases, with order parameter values near unity. At $\alpha \approx 1$ they start to lose synchronization and, for α greater than a critical value of *circa* 2.0 the order parameter assumes small values, which we assume going to zero as the lattice size becomes infinite, as before. In Fig. 4(d) this transition is shown to occur only if the coupling strength is large enough.

The three numerical diagnostics we have used to describe phase and frequency synchronization of bursting neurons converge to a common picture, in which the synchronization is promoted by a combination of low values of the range parameter α (or couplings where a large number of neighbors are taken into account) and large enough coupling strength ϵ. The two limiting cases are: (i) mean-field strong coupling, where all sites contribute to the coupling in the same proportion through their mean field resulting in a synchronized state; and (ii) nearest-neighbor weak

coupling, where synchronization does not happen at all. The in-between behavior can be qualitatively understood by comparing two opposite tendencies: one of them is the intrinsic randomness of the frequencies caused by the assumed fluctuation of neuron parameters, which inhibits synchronization. The other one is the coupling effect, which leads to the adjustment of the bursting phases, so facilitating synchronization. The actual behavior of the network is the outcome of the competition between such conflicting tendencies.

The existence of a synchronization process, although governed by a tradeoff between coupling/diffusion and randomness/inhomogeneity, is chiefly a collective effect, a property which emerges from the complexity inherent to the chaotic spatio-temporal dynamics of the coupled map lattice. One example is the existence of a phase transition when α is near zero and ϵ increases past a critical value.

5. External phase synchronization

Once a neuron ensemble burst in synchrony we may investigate the effect of an external time-periodic signal. Such a perturbation, when applied to an ensemble of first-order phase oscillations, has been shown to produce global phase locking [29], and it has been observed in lattices of Rulkov neurons with global [19] and scale-free coupling [21]. We have implemented this procedure by adding external time-periodic interventions to the power-law lattice (5)–(6). An external harmonic signal is applied to one selected neuron $i = S$ (the remaining neurons other unchanged) in the following way

$$x_{n+1}^{(S)} = \frac{\theta^{(S)}}{1 + \left(x_n^{(S)}\right)^2} + y_n^{(S)} + \frac{\epsilon}{\eta(\alpha)} \sum_{j=1, j\neq i}^{N'} \frac{1}{j^\alpha} \left[x_n^{(S+j)} + x_n^{(S-j)}\right] + d\sin(\omega n), \tag{12}$$

where d and ω are the external signal amplitude and frequency, respectively, and the site S in principle can be anyone chosen at random in the network. We shall also consider situations where more than one neuron is acted upon, with a signal with the same amplitude and frequency as in Eq. (12).

We have used coupling strength values for which the unperturbed lattice ($d = 0$) exhibits bursting synchronization. When both the amplitude and frequency of the external time-periodic signal are nonzero, the neuron bursting frequencies $\Omega^{(i)}$ lock approximately at a common value, as depicted in Fig. 5(a), where the frequency mismatch $\Omega^{(i)} - \omega$ is plotted against ω for all neurons belonging to a given lattice. They exhibit a common locking region centered at $\approx$0.0155, with essentially the same behavior at both sides of the locking interval. When the applied frequency lies outside this mode-locking interval, the bursting rhythms of all sites are still synchronized, but at other frequencies than the externally applied one. When the signal amplitude is increased, the locking interval is enlarged to approximately the same width for all neurons, but their behavior outside the interval varies considerably, specially for higher frequencies (Fig. 5(b)). It is important to observe that this effect exhibits a saturation for large signal amplitudes, since the locking interval may not exist at all (Fig. 5(c)).

Another noteworthy feature depicted in Fig. 5(b) and (c) is that, for driving frequencies ω higher than those values yielding mode locking, and provided the coupling strength is large enough, the bursting frequencies become different for each neuron. In other words, the application of an external signal with high frequency is capable to destroy the bursting synchronized state that existed before the application of the signal. This has potential applications in the control of certain pathological rhythms in the brain [22,30,31].

According to Ref. [19] the bursting phase synchronization is possible due to the coupling effect on the triggering or termination of a burst in the individual neurons. A burst can be terminated (the neuron is driven to a quiescent state) if the external signal is positive. Conversely, a burst can be delayed if the signal is negative. The combination of these effects leads to the synchronization of the driven neuron with the signal. The effect of coupling, once it takes into account the mutual influences of all lattice sites, is to change the mean field that each neuron feels. In the case of a power-law coupling, distant sites contribute less to coupling. Hence, the more local the coupling is (large α) the less a distant neuron feels the synchronization effect caused by the signal on the driven neuron. Hence we expect worse synchronization properties as α increases, and no synchronization at all for nearest-neighbor couplings ($\alpha \to \infty$).

The frequency-locking interval is a cross-section of an Arnold-like tongue in the parameter plane amplitude *versus* frequency of the external driving signal (Fig. 6(b)). This tongue is clearly asymmetric for small amplitudes, for its left boundary is steeper than the right one, becoming more symmetric as the signal amplitudes are higher, as long as they do not exceed the saturation limit. In order to characterize quantitatively this asymmetry we define the width of

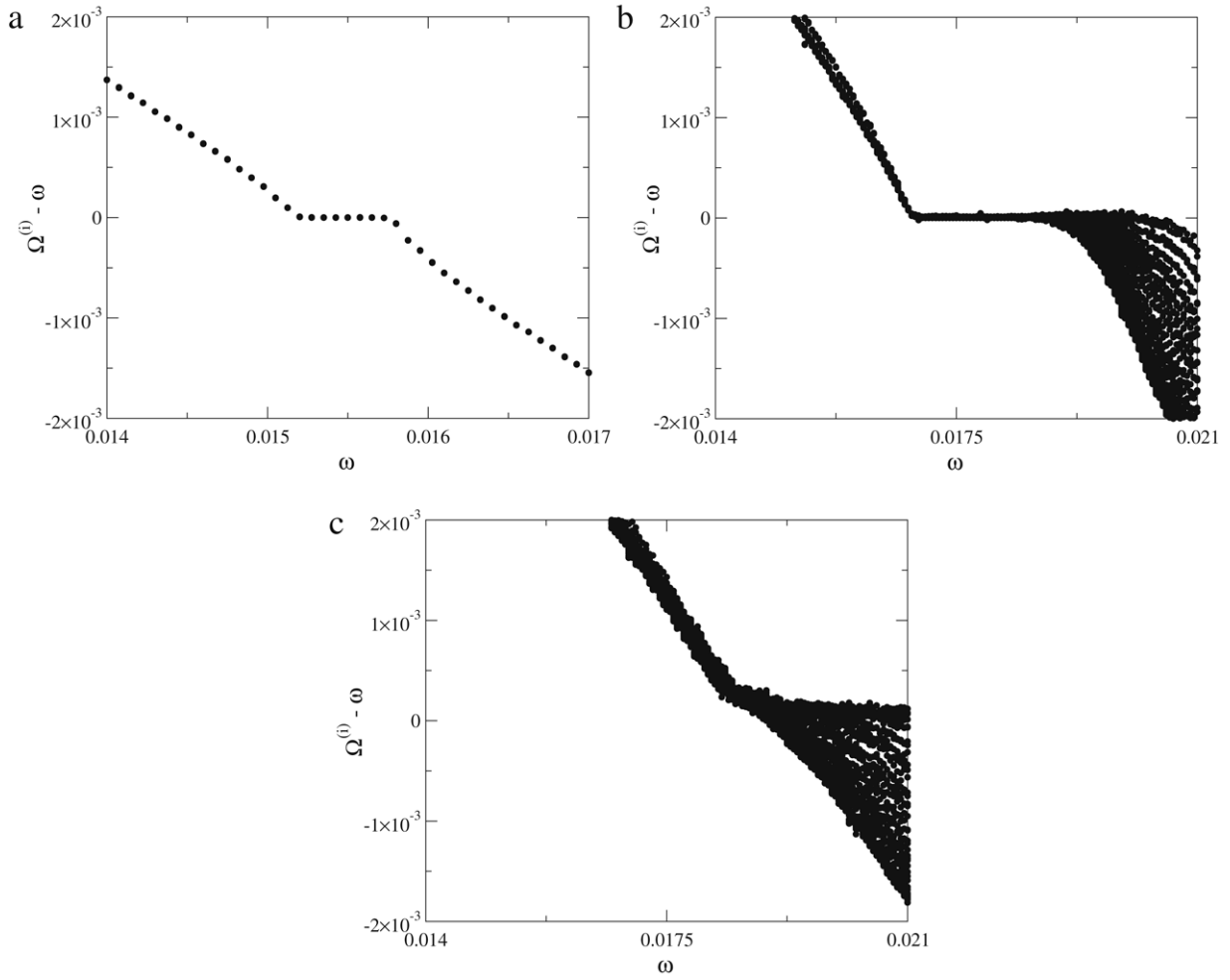

Fig. 5. Frequency mismatch of bursting neurons *versus* the external driving frequency for a lattice with $N = 51$ neurons, $\alpha = 0.15$, $\epsilon = 0.1$, and a driving signal applied at the site $S = 1$ with amplitude (a) $d = 0.05$, (b) $d = 2.0$, and (c) $d = 4.0$.

this locking interval $\Delta\omega$, and also the interval width $\delta\omega$ counted only from the unperturbed frequency (i.e. at $d = 0$) (Fig. 6(a)). The former increases with the signal amplitude initially with a small rate, then more rapidly (provoking the above-mentioned asymmetry), and finally at a slower rate.

The dependence of the width with the amplitude can be fitted by a power-law $\Delta\omega \sim d^{\varpi}$, where $\varpi = 1.750 \pm 0.040$ for the fast-rate region, and $\varpi = 0.317 \pm 0.004$ for the slow-rate region (Fig. 6(c)). The asymmetry of the tongue manifests itself in two similar regimes for the part of the tongue to the right of the zero-signal, or $\delta\omega \sim d^{\varsigma}$, where $\varsigma = 1.480 \pm 0.040$ for the fast-rate region, and $\varsigma = 0.199 \pm 0.004$ for the slow-rate region (Fig. 6(d)).

The wider the frequency-locking interval is, the more robust is the external driving with respect to imperfect parameter determination and noise, which is a question of considerable experimental importance. However, it may well happen that, if only one pinning (i.e., a driving applied on only one neuron) is considered, the corresponding locking interval would be too small so as to ensure robustness against imperfect parameter determination. For example, if the frequency of the pinning is known up to an uncertainty comparable to the tongue width, it would be rather difficult to achieve mode locking. On the other hand, simply increasing the amplitude of a single pinning may not produce the desired result, since it would lead to saturation (see Fig. 5(c)).

The latter problem is particularly severe when the lattice size increases, as illustrated by Fig. 7, where we plot the locking interval width as a function of the inverse lattice size. If only one pinning is used, the tongue width decreases with the lattice size in a nearly linear fashion, Hence it would be difficult to obtain mode locking in large

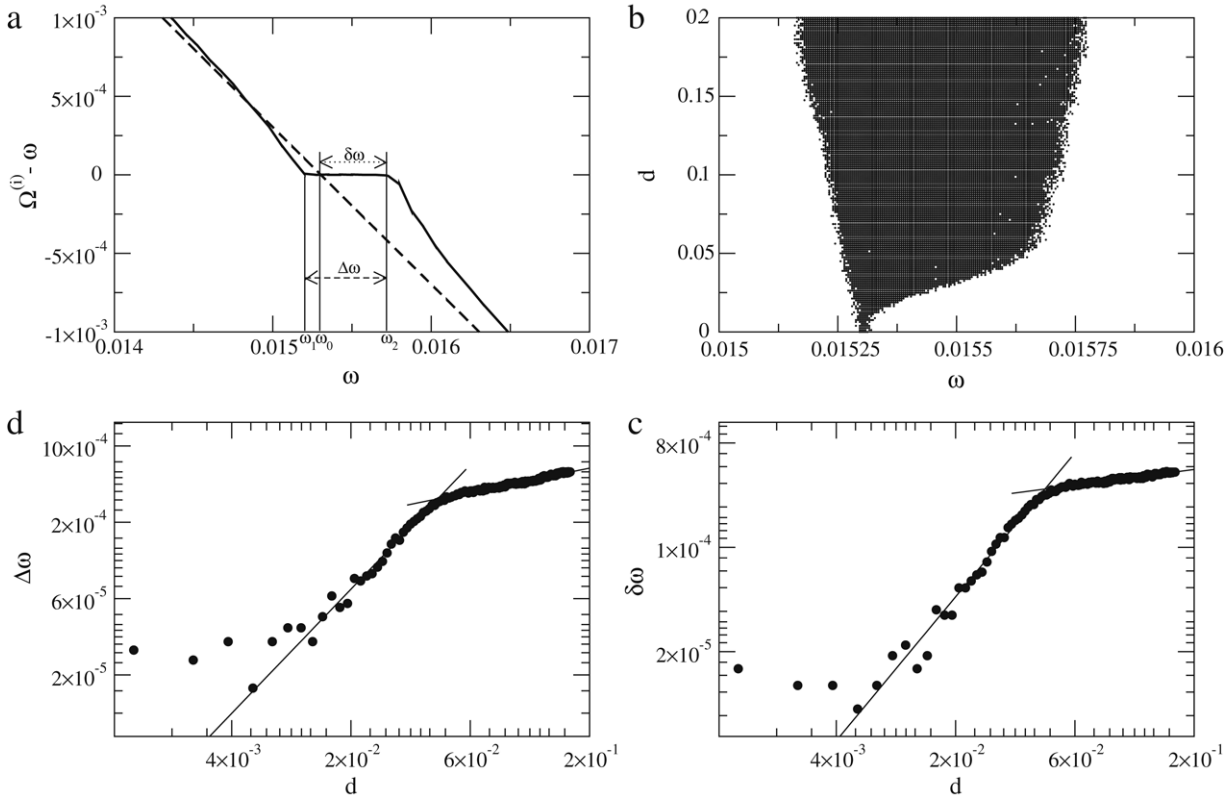

Fig. 6. Mode locking for a lattice with $N = 51$ neurons, $\alpha = 0.5$, $\epsilon = 0.07$, driving signal applied at the site $S = 1$. (a) Frequency mismatch of bursting neurons *versus* the external driving frequency for amplitude $d = 0$ (dashed line) and $d = 0.07$ (full line). (b) Mode-locking tongue in the amplitude *versus* frequency of the driving signal. (c) Full width of the mode-locking tongue as a function of the driving amplitude. (d) The same as (c) for the partial width (to the right and with respect to the $d = 0$ intercept). The full lines in (c) and (d) are least-squares fits (see text for details).

ensembles. One possible way to circumvent this problem is to use more than one site to control at the same time (multiple pinnings) [19]. As depicted in Fig. 7, the tongues dilate as the number of pinnings (N_p) is augmented, and the dependence on the lattice size is more pronounced, fitted by similar scaling laws in the form $\Delta\omega \sim N^{-1}$. This result has been observed for a number of pinnings between 1 and 4, applied at randomly chosen neurons, with the same amplitude and frequency of the single pinning case. For a given lattice size N, the tongue width increases with the number of pinnings, but this effect is more pronounced for small lattices than for larger ones.

6. Conclusions

A coupled map lattice constructed with neurons obeying a discrete-time process (Rulkov map) can display many features expected in complex networks of biological neurons. One of them is that the coupled neurons can burst synchronously, i.e. their bursting activity starts at approximately the same time for all neurons, even though they have slightly different parameters and could not exhibit this effect by mere chance. A one-dimensional lattice with non-local coupling is necessary to emulate aspects of the complex architecture of actual assemblies of neurons. A commonly used model is a global, or mean-field lattices, where each neuron interacts with all other sites in the same way, regardless of the distance between them. However, in actual networks some dependence on the distance is necessary due to the spatial dependence of the neurophysiological processes involved in synaptical coupling.

We demonstrated the possibility of obtaining bursting synchronization of Rulkov neurons in a non-locally coupled lattice, where the coupling strength decreases with the lattice distance in a power-law fashion. Since, in our model, we recover the results obtained for mean-field global lattices (in the limit of vanishing range parameter), our work generalizes the previous one by Ivanchenko and co-workers [19]. The novelty introduced by considering the variable effective range lies in the strong dependence of the synchronization properties on the coupling parameters.

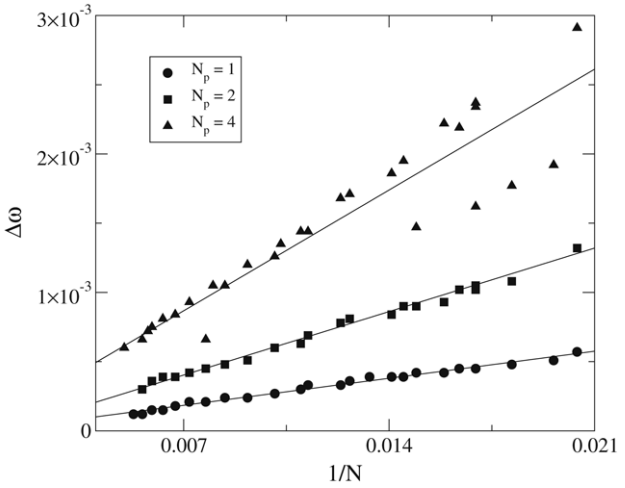

Fig. 7. Width of the frequency-locking interval *versus* inverse lattice size for different number of driving inputs, all of them with the same amplitude $d = 0.20$, in a lattice with $\alpha = 0.5$ and $\epsilon = 0.1$.

We found that bursting synchronization occurs more likely if the coupling range approaches that of the mean-field case. This is due to the competition between the intrinsic randomness of the bursting frequencies originating from the diversity of neuron parameters, and the diffusive effect caused by coupling. Synchronization is facilitated since the less the range parameter, the more the distant neurons contribute to coupling. The general features of this behavior are similar to those observed in a generalized Kuramoto model, where a transition is found, as the range parameter is varied past a critical value [32].

Once the bursting activity of the network is synchronized, we also investigated under which conditions we obtain mode locking of the synchronized behavior by applying a localized time-dependent signal with amplitude and frequency. We observed that the locking frequency interval width increases with the signal amplitude, as long as the latter does not exceed a saturation threshold, above which there is no longer frequency locking. In terms of the parameter plane this defines an asymmetric Arnold-like tongue. Since real neuron networks typically have a huge number of units, and the width of the frequency-locking tongue was found to decrease with the lattice size (depending linearly with $1/N$), we found it useful to employ multiple pinnings.

Finally, if the external signal frequency exceeds those values yielding mode locking we are able to destroy bursting synchronization. In situations where synchronization is undesirable, e.g. when related to pathological brain rhythms, the application of a time-periodic external signal may become a procedure of controlling such abnormal rhythms [22,30,31].

Acknowledgments

This work was made possible with the help of CNPq, CAPES, and Fundação Araucária (Brazilian Government Agencies).

References

[1] M.F. Bear, B.W. Connors, M.A. Paradiso, Neuroscience: Exploring the Brain, 2nd ed., Lippincott Williams & Wilkins, Philadelphia, 2002.
[2] J.J. Hopfield, Proc. Natl. Acad. Sci. USA 79 (2254) (1982);
J.J. Hopfield, D.W. Tank, Science 233 (1986) 625.
[3] H. Gutfreund, Physica A 163 (1990) 373.
[4] W.S. Pritchard, D.W. Duke, Int. J. Neurosci. 67 (1992) 31;
W.J. Freeman, Int. J. Bifurcation Chaos 2 (1992) 451;
S.J. Schiff, K. Jerger, D.H. Duong, T. Chang, M.L. Spano, W.L. Ditto, Nature 370 (1994) 615;
S.N. Sarbadhikari, K. Chakrabarty, Med. Engineer. Phys. 23 (2001) 445;
For a different perspective see also K. Lehnertz, C.E. Elger, J. Arnhold, P. Grassberger (Eds.), Chaos in Brain? World Scientific, Singapore, 2000.

[5] A.L. Hodgkin, A.F. Huxley, J. Physiol. 116 (1952) 449;
A.L. Hodgkin, A.F. Huxley, J. Physiol. 117 (1952) 500.
[6] R.A. FitzHugh, Biophys. J. 1 (1961) 445;
J. Nagumo, S. Arimoto, S. Yoshizawa, Proc. IRE 50 (1962) 1061.
[7] J.L. Hindmarsch, R.M. Rose, Philos. Trans. R. Soc. London, Ser. B 221 (1984) 87.
[8] G. Tanaka, B. Ibarz, M.A.F. Sanjuan, K. Aihara, Chaos 16 (2006) 13113.
[9] H. Nozawa, Chaos 2 (1992) 377;
S. Ishii, M. Sato, Physica D 121 (1998) 344.
[10] I. Belykh, E. de Lange, M. Hasler, Phys. Rev. Lett. 94 (2005) 188101.
[11] S. Coombes, P.C. Bressloff (Eds.), Bursting: The Genesis of Rhythm in the Nervous System, World Scientific, Singapore, 2005.
[12] D. Chialvo, Chaos Solitons Fractals 5 (1995) 461;
D.R. Chialvo, Physica A 340 (2004) 756;
O. Sporns, D.R. Chialvo, M. Kaiser, C.C. Hilgetag, Trends Cogn. Sci. 8 (2004) 418;
V.M. Eguiluz, D.R. Chialvo, G.A. Cecchi, M. Baliki, A.V. Apkarian, Phys. Rev. Lett. 94 (2005) 18102.
[13] N.F. Rulkov, Phys. Rev. Lett. 86 (2001) 183.
[14] A.J. Pellionisz, in: E. Rodney, M.J. Cotterill (Eds.), Models of Brain Function, Cambridge University Press, Cambridge, 1989;
F. Caserta, W.D. Eldred, E. Fernandez, R.E. Hausman, L.R. Stanford, S.V. Bulderev, S. Schwarzer, H.E. Stanley, J. Neurosci. Meth. 56 (1995) 133;
E. Bieberich, Biosystems 66 (2002) 145.
[15] B. Roerig, B. Chen, Cereb. Cortex 12 (2002) 187.
[16] S. Raghavachari, J.A. Glazier, Phys. Rev. Lett. 74 (1995) 3297.
[17] C. Wagner, R. Stoop, Int. J. Bifurcation Chaos 17 (2008) 3409.
[18] A.M. Thomson, Current Biol. 10 (2000) R110.
[19] M.V. Ivanchenko, G.V. Osipov, V.D. Shalfeev, J. Kurths, Phys. Rev. Lett. 93 (2004) 134101.
[20] M.G. Rosenblum, A.S. Pikovsky, J. Kurths, Phys. Rev. Lett. 76 (1996) 1804.
[21] C.A.S. Batista, A.M. Batista, J.C.A. de Pontes, R.L. Viana, S.R. Lopes, Phys. Rev. E 76 (2007) 16218.
[22] M. Rosenblum, A. Pikowsky, Phys. Rev. E 70 (2004) 41904.
[23] M. Dhamala, V.K. Jirsa, M. Ding, Phys. Rev. Lett. 92 (2004) 28101.
[24] N.F. Rulkov, Phys. Rev. E 65 (2002) 41922;
N.F. Rulkov, I. Timofeev, M. Bazhenov, J. Comp. Neurosci. 17 (2004) 203.
[25] P. Dayan, L. F, Theoretical Neuroscience: Computational and Mathematical Modeling of Neural Systems, MIT Press, Cambridge, 2001.
[26] A.F. Rozenfeld, R. Cohen, D. ben-Avraham, S. Havlin, Phys. Rev. Lett. 89 (2002) 218701.
[27] S.E. de S Pinto, R.L. Viana, Phys. Rev. E 61 (2000) 5154;
S.E. de S Pinto, S.R. Lopes, R.L. Viana, Physica A 303 (2002) 339.
[28] Y. Kuramoto, Chemical Oscillations, Waves, and Turbulence, Springer Verlag, Berlin, 1984.
[29] H. Sakaguchi, Prog. Theor. Phys. 79 (1988) 39.
[30] J. Milton, P. Jung (Eds.), Epilepsy as a Dynamic Disease, Springer Verlag, Berlin, 2003.
[31] A. Behabid, et al., Lancet 337 (1991) 403.
[32] J.L. Rogers, L.T. Wille, Phys. Rev. E 54 (1996) R2193.